

## THE $^{11}\text{B}/^{10}\text{B}$ RATIO OF LOCAL INTERSTELLAR DIFFUSE CLOUDS<sup>1</sup>

DAVID L. LAMBERT AND YARON SHEFFER

Department of Astronomy, University of Texas at Austin, Austin, Texas 78712

S. R. FEDERMAN

Department of Physics and Astronomy, University of Toledo, Toledo, OH 43606

JASON A. CARDELLI<sup>2</sup> AND ULYSSES J. SOFIA

Astronomy and Astrophysics, Mendel Hall, Villanova University, Villanova, PA 19085

AND

DAVID C. KNAUTH

Department of Physics and Astronomy, University of Toledo, Toledo, OH 43606

Received 1997 June 12; accepted 1997 September 29

### ABSTRACT

The isotopic ratio  $^{11}\text{B}/^{10}\text{B}$  of gas in diffuse interstellar clouds toward  $\zeta$  Oph,  $\kappa$  Ori, and  $\delta$  Sco is measured using *HST*/Goddard High Resolution Spectrograph echelle spectra of the B II 1362 Å line. To within the errors of measurement, the three lines of sight give identical results for a mean value of  $^{11}\text{B}/^{10}\text{B} = 3.4 \pm 0.7$ , a value quite similar to the solar system ratio of 4.05. These results show that the latter value is not highly anomalous and that a ratio higher than 2.5, as predicted for boron produced from spallation reactions controlled by high-energy cosmic rays, most probably requires a general explanation. The observed ratio is consistent with additional boron production either by spallation by low-energy (“Orion”) cosmic rays or by neutrino-induced spallation of carbon in Type II supernovae. The total abundance of B in the diffuse clouds is a factor of 5 less than the meteoritic value. This depletion of B is consistent with that found for Cu and Ga, two elements with a condensation temperature similar to B.

*Subject headings:* dust, extinction — ISM: abundances — ultraviolet: ISM

### 1. INTRODUCTION

In the inventory of processes that comprise contemporary ideas about the origins of the chemical elements, two may account for production of  $^{10}\text{B}$  and  $^{11}\text{B}$ , the stable isotopes of boron. The process with the longer theoretical bloodline involves spallation reactions between cosmic rays and interstellar nuclei. Under present conditions in the interstellar medium, the dominant contribution comes from cosmic-ray protons colliding with interstellar oxygen nuclei (Reeves, Fowler, & Hoyle 1970). The second process is neutrino-induced spallation occurring in Type II supernovae: neutrinos streaming out from the collapsed core interact with  $^{12}\text{C}$  in the carbon-rich shell to produce unstable  $^{11}\text{C}$  that decays to  $^{11}\text{B}$  (Woosley et al. 1990). Since neutrino-induced spallation produces  $^{11}\text{B}$  but not  $^{10}\text{B}$ , and spallation driven by cosmic rays produces both stable isotopes, observations of the boron isotopic ratio are a potential monitor of the relative importance of the two schemes for synthesis of boron. In placing the emphasis on production, the assumption is made that, in gas returned to the interstellar medium by stars—Type II supernovae excepted—boron has been effectively completely destroyed such that the boron isotopic ratio is unaffected by recycling of gas back to the interstellar medium.

The predicted isotopic ratio,  $^{11}\text{B}/^{10}\text{B}$ , from spallation by cosmic rays depends on the energy spectrum of the cosmic

rays (primarily the protons and  $\alpha$ -particles), the composition of the cosmic rays and the interstellar gas, and the spallation cross sections. Calculations (see Meneguzzi, Audouze, & Reeves 1971; Reeves 1974) predict a ratio  $^{11}\text{B}/^{10}\text{B}$  of about 2.5, in conflict with the observed ratio in the solar system (the Earth, meteorites, and lunar rocks) for which the ratio  $^{11}\text{B}/^{10}\text{B}$  is about 4 (Anders & Grevesse 1989; Chaussidon & Robert 1995; Zhai et al. 1996). These early calculations also predicted the abundance ratio B/Be to be below that measured for the solar system. Beryllium and  $^6\text{Li}$  are key nuclides as cosmic-ray spallation is the sole mode of synthesis for them; their abundances effectively calibrate the cosmic-ray flux and its variation over the life of the Galaxy. By crafting the cosmic-ray energy spectrum appropriately at energies around the differing thresholds for  $^{11}\text{B}$  and  $^{10}\text{B}$  production, it was possible to raise the predicted isotopic ratio from 2.5 to 4 (Meneguzzi & Reeves 1975). Invocation of low-energy cosmic rays also raised the predicted elemental abundance ratio B/Be closer to that measured for meteorites. Very recently, evidence of a flux of such low-energy cosmic rays in the Orion association (Bloemen et al. 1994) has suggested that low-energy C and O cosmic rays may deserve careful reconsideration. Since  $^{11}\text{B}$  but neither  $^{10}\text{B}$  nor Be may be produced in Type II supernovae, it is possible to raise the  $^{11}\text{B}/^{10}\text{B}$  and B/Be ratios by allowing supernovae to supplement the products from cosmic-ray spallation without invoking a flux of low-energy cosmic rays.

These competing theoretical ideas about the  $^{11}\text{B}/^{10}\text{B}$  ratio developed at a time when there was but one observational datum: the isotopic ratio for the solar system. Although rather complementary information is obtainable from the elemental B/Be ratio, there was also a dearth of

<sup>1</sup> Based on observations obtained with the NASA/ESA *Hubble Space Telescope* through the Space Telescope Science Institute, which is operated by the Association of Universities for Research in Astronomy, Inc., under NASA contract NAS4-26555.

<sup>2</sup> Deceased.

data on stellar (or interstellar) abundances of Be/H and especially on B/H. The observational situation is now greatly improved for the elemental abundances. It is the principal purpose of this paper to present results for the  $^{11}\text{B}/^{10}\text{B}$  ratio in local interstellar diffuse clouds. A preliminary discussion based on a measurement for one line of sight was given by Federman et al. (1996).

## 2. OBSERVATIONS AND ANALYSIS

### 2.1. Introduction

In interstellar diffuse clouds, boron is overwhelmingly present as the ion  $\text{B}^+$ . The strongest resonance line of  $\text{B}^+$  is at 1362.461 Å, with an oscillator strength  $f = 0.98$  (Morton 1991). A large-scale theoretical calculation accurate to 1% predicts the  $^{10}\text{B}$  line to be shifted by 13.3 mÅ to longer wavelengths of the  $^{11}\text{B}$  line (Jönsson, Johansson, & Froese Fischer 1994). There are no laboratory measurements of the shift, but a confirming determination from *Hubble Space Telescope* (*HST*) spectra was reported by Federman et al. (1996). Since the turbulent velocity in a diffuse cloud is smaller than the isotopic shift of 2.93 km s $^{-1}$ , an observation of the B II line in absorption from a single cloud would, if made at very high spectral resolution, show the (presumably) weaker  $^{10}\text{B}$  line resolved from the  $^{11}\text{B}$  line. This ideal observation is compromised in practice by two factors: (1) the highest resolution available using the *HST*, presently the only facility providing a capability for ultraviolet spectroscopy, is approximately 4 km s $^{-1}$ ; (2) there are multiple clouds along almost all lines of sight for which the column density of  $\text{B}^+$  ions is sufficiently high to provide a detectable absorption line at 1362 Å. Nonetheless, simulations of line profiles as observed with the highest available resolution on *HST* indicated that the boron isotopic ratio would be measurable to an interesting precision with the Goddard High Resolution Spectrograph (GHRS) in its echelle mode.

In the echelle mode, clouds with velocity separations of less than a few km s $^{-1}$  will not be resolved. Unrecognized overlapping of clouds could quite obviously result in spurious determinations of the boron isotopic ratio from the B II line at 1362 Å. In order to account for overlapping clouds, observations of a Cu II line at 1358 Å and a Ga II line at 1414 Å were also obtained. The ions  $\text{B}^+$ ,  $\text{Cu}^+$ , and  $\text{Ga}^+$  are

expected to show similar distributions along a line of sight because each is the dominant ion of its element in diffuse clouds, and each element is incorporated into grains to a similar level. In the analysis, the observed Cu II and Ga II profiles serve as “templates” for the unresolved profile of the B II lines. Neither the Cu II nor the Ga II lines are expected to show appreciable isotopic or hyperfine splitting. The isotopic ratio is determined by fitting the observed B II 1362 Å profile using a template profile and adjusting the  $^{11}\text{B}/^{10}\text{B}$  ratio to obtain the optimum fit.

### 2.2. Observations

Observations of three stars— $\zeta$  Oph,  $\kappa$  Ori, and  $\delta$  Sco—were obtained using the GHRS with the ECH-A grating and the small science aperture (SSA), providing a nominal resolution of 4 km s $^{-1}$ . Boron is a trace element, and as such the B II 1362 Å line is inevitably weak for the column densities of diffuse clouds that may be probed by bright hot stars. Kappa Ori and  $\zeta$  Oph were selected because the B II line had been detected previously (Meneguzzi & York 1980; Federman et al. 1993). No previous detection of the 1362 Å line was known for  $\delta$  Sco, but the reported column density of neutral hydrogen suggested that the line would be of a useful strength. In fact, the equivalent width of the line is nearly twice that seen toward  $\zeta$  Oph and  $\kappa$  Ori.

Two settings of ECH-A were used: one provides the 1414 Å Ga II line and the other the 1362 Å B II and 1358 Å Cu II lines. The data were obtained using an observing strategy that included four samples per diode width, a four position comb addition that reduces diode-to-diode variations, and four slightly different carousel positions for the observations (FP-SPLIT = 4). Each carousel grating shift moved the spectrum approximately nine diodes in the dispersion direction on the detector array. This procedure allows fixed pattern noise to be well defined and removed from the final co-added spectra. Because of the weakness of the  $^{10}\text{B}$  absorption features, high signal-to-noise spectra were necessary. We therefore followed the iterative noise removal procedures of Cardelli & Ebbets (1994). The final co-added spectra show the sharp interstellar lines superposed on an undulating spectrum of broad stellar lines. The three interstellar lines in the observed stars are shown in Figure 1 for a region of about  $\pm 1$  Å about the line. The signal-to-noise ratio (S/N) per  $\frac{1}{4}$  diode in the continuum near the lines is

TABLE 1

SUMMARY OF THE OBSERVATIONS

Star	Date	Rootname <sup>a</sup>	$\lambda$ (Å)	Exposure Time (s)	S/N <sup>b</sup>	Species
$\delta$ Sco .....	1995 Aug 12	z2u70207t[8]	1360.16	652.8	...	Cu II, B II
		z2u70208t[7]	1360.71	524.8	299	
		z2u70209t[8]	1412.09	870.4	...	Ga II
		z2u7020at[8]	1412.63	652.8	311	
$\kappa$ Ori .....	1996 Feb 21	z2u70109t[4]	1360.30	435.2	...	Cu II, B II
		z2u7010at[7]	1360.84	524.8	403	
		z2u7010bt[8]	1412.49	652.8	...	Ga II
		z2u7010ct[8]	1413.02	652.8	328	
$\zeta$ Oph.....	1996 Apr 18	z2u70307t[8]	1360.50	1479.8	...	Cu II, B II
		z2u70308t[8]	1361.05	1523.2	...	
		z2u70309t[8]	1361.32	1523.2	345	
		z2u7030at[4]	1412.45	1088.0	...	Ga II
		z2u7030dt[4]	1412.97	1088.0	...	
		z2u7030et[4]	1413.24	1196.8	357	

<sup>a</sup> Brackets indicate number of FP-SPLIT subexposures.

<sup>b</sup> Resultant ratio after exposure co-addition.

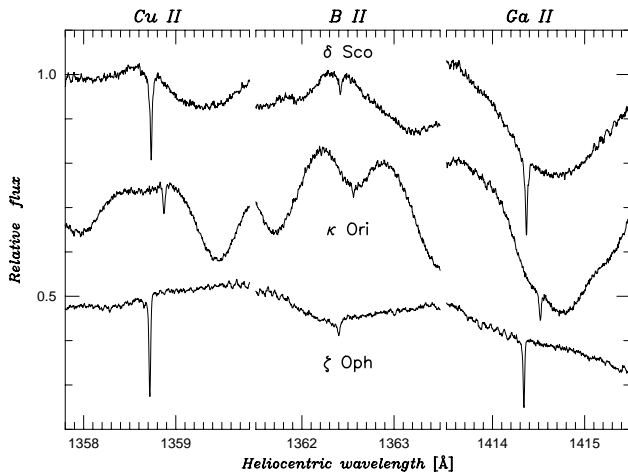


FIG. 1.—Interstellar lines of Cu II, B II, and Ga II in the spectra of  $\delta$  Sco,  $\kappa$  Ori, and  $\zeta$  Oph. The sharp interstellar lines are seen superposed on the undulating stellar spectrum.

given in Table 1, which lists rootnames and other information.

Interstellar lines are compared and analyzed using rectified spectra. A local continuum, defined by a low-degree polynomial fitted to a region around the line of interest, is divided into the observed spectrum to obtain the rectified spectrum. Equivalent widths of the lines are given in Table 2.

### 3. ANALYSIS

The Cu II and Ga II profiles serve as templates for analysis of the B II line. Direct application of the former profiles is inappropriate as the line cores are partially saturated. Note that the Cu II and Ga II lines have similar equivalent widths and that these are stronger than the B II line. An rms-minimizing code was used to fit a synthetic profile to an observed profile for the Cu II and Ga II lines. The former was constructed from one or more overlapping components for which the absorption coefficient was assumed to have a Voigt profile. In effect, the profile is a Gaussian as the observed lines are too weak for the radiatively damped Lorentzian wings to be a factor. The number of components was chosen by inspection of the Cu II and Ga II lines:  $\delta$  Sco has three obvious components,  $\zeta$  Oph has two, and one seems adequate for  $\kappa$  Ori. The components are defined by their width (the familiar  $b$ -parameter,  $b$  in  $\text{km s}^{-1}$ ), a column density ( $N$  in  $\text{cm}^{-2}$ ), and a velocity separation ( $\Delta v$  in  $\text{km s}^{-1}$ ) between components. The instrumental profile

TABLE 2  
EQUIVALENT WIDTHS,  $W_\lambda^a$

STAR	$W_\lambda^a$		
	B II (1362 Å)	Cu II (1358 Å)	Ga II (1414 Å)
$\zeta$ Oph .....	$0.6 \pm 0.2$	$6.4 \pm 0.5^b$	$4.4 \pm 0.3^b$
$\kappa$ Ori .....	$0.7 \pm 0.2$	$1.7 \pm 0.2$	$1.5 \pm 0.2$
$\delta$ Sco .....	$1.3 \pm 0.3$	$7.1 \pm 0.4^b$	$6.5 \pm 0.3^b$

<sup>a</sup> Values derived from synthetic fits to data.

<sup>b</sup> These  $W_\lambda$  include a blue component that is not part of the B II analysis.

was represented by a Gaussian corresponding to the resolution  $R = \lambda/\delta\lambda = 80,000$ . Synthetic spectra were convolved with the instrumental profile before comparison with an observed profile. Column densities are computed from the integrated line profiles using the  $f$ -values:  $f = 0.38$  for Cu II 1358 Å and  $f = 1.80$  for Ga II 1414 Å (Morton 1991).

Comparison of observed and synthetic spectra utilized a rms-minimizing code (Y. Sheffer, unpublished) in which the adjustable parameters in the synthesis were changed in shrinking step sizes, and only those that decrease the overall deviation from the observed spectrum were retained. The lines of Cu II and Ga II were the first to be fitted by the rms-minimizing code, yielding Doppler  $b$ -parameter and column density ratios for all the Voigt components that make up the entire profile. Such Cu II and Ga II output become the input for the B II fits; i.e.,  $b$ -values and component ratios were not redetermined for B II. For the stronger B II absorption toward  $\delta$  Sco and  $\zeta$  Oph, the code was used for determining the column density, radial velocity, and isotopic ratio for the line profile. For the weaker B II line of  $\kappa$  Ori, the velocity could not be determined by the fitting code. It was then necessary to adopt the radial velocity of the Cu II line on the same spectrum and fit only the column density and isotopic ratio. In the case of  $\delta$  Sco, it was possible to enter the isotopic wavelength shift as an adjustable parameter: the result of  $13.7 \pm 3.5$  mÅ (Federman et al. 1996) is in excellent agreement with the accurate theoretical prediction (Jönsson et al. 1994), which was taken as a nonadjustable splitting for the analyses of the B II line in the other two stars.

Since both Cu II and Ga II serve as profile templates, they were used independently to fit the B II line. The final estimate of the  $^{11}\text{B}/^{10}\text{B}$  ratio is a weighted mean of the two results. Weights are inversely proportional to the squares of the error bars of the ratios from each fit. The error bars for the ratios were computed directly from the uncertainties in the equivalent widths of both isotopes.

Estimates of error bars for the adjustable parameters were tied to the primary observational uncertainty, which was taken to be the error in the measured equivalent width of the line profile—see Table 2. Any derived uncertainty in synthesis parameters thus represents these observational errors as solely due to each parameter's error bars; hence, these are certainly conservative estimates. Determination of uncertainties was quantified by means of equal rms deviations as representing equal profile deviations for differing parameters. For the stronger Cu II and Ga II lines (in  $\zeta$  Oph and  $\delta$  Sco), the column density uncertainty amounts to  $\sim 6\%$ . Other error bars are  $\pm 0.2$   $\text{km s}^{-1}$  in  $\Delta v$  and  $\pm 0.2$   $\text{km s}^{-1}$  in  $b$ . A larger uncertainty of  $\sim 12\%$  in the column densities toward  $\kappa$  Ori is accompanied by larger error bars of  $\pm 0.4$   $\text{km s}^{-1}$  in  $\Delta v$  and  $\pm 0.7$   $\text{km s}^{-1}$  in  $b$ . Fractional column densities are uncertain at a level of  $\pm 0.05$  in  $\log N$ .

Results from the fits to the Cu II and Ga II lines are summarized in Table 3. Observed and synthetic profiles are shown in Figures 2 ( $\zeta$  Oph), 3 ( $\kappa$  Ori), and 4 ( $\delta$  Sco). Observed and best-fitting synthetic B II profiles are shown for  $\zeta$  Oph and  $\kappa$  Ori in Figure 5 and 6, respectively. Figure 7 shows the profiles for  $\delta$  Sco—see also Federman et al. (1996). Final results for the isotopic ratio are given in Table 4. As a guide to the uncertainty over the ratio,  $\delta$  Sco's B II line is shown in Figure 8 with three superposed synthetic profiles. One synthetic profile is that provided by the fitting

TABLE 3  
PROFILE ANALYSIS OF THE Cu II AND Ga II LINES

STAR	FIT	COMPONENT 1 <sup>a</sup>		COMPONENT 2			COMPONENT 3			$N_i/10^{10}$
		$N_1/N_t$	$b$	$N_2/N_t$	$b$	$\Delta v$	$N_3/N_t$	$b$	$\Delta v$	
$\zeta$ Oph.....	Ga	0.90	0.47	0.10	2.2	-5.5	...	...	...	16
	Cu	0.91	0.89	0.09	2.8	-5.1	...	...	...	120
$\kappa$ Ori.....	Ga	1.00	2.4	...	...	...	...	...	...	4.7
	Cu	1.00	2.6	...	...	...	...	...	...	28
$\delta$ Sco.....	Ga	0.40	0.58	0.40	3.8	-3.1	0.14	1.5	+5.0	22
	Cu	0.62	0.52	0.22	2.0	-3.8	0.16	2.2	+4.2	123

<sup>a</sup> The fitted parameters are the fractional column density  $N_i/N_t$ , the Doppler parameter  $b$  in  $\text{km s}^{-1}$ , and the velocity difference  $\Delta v$  in  $\text{km s}^{-1}$  of the component relative to the velocity of component 1.

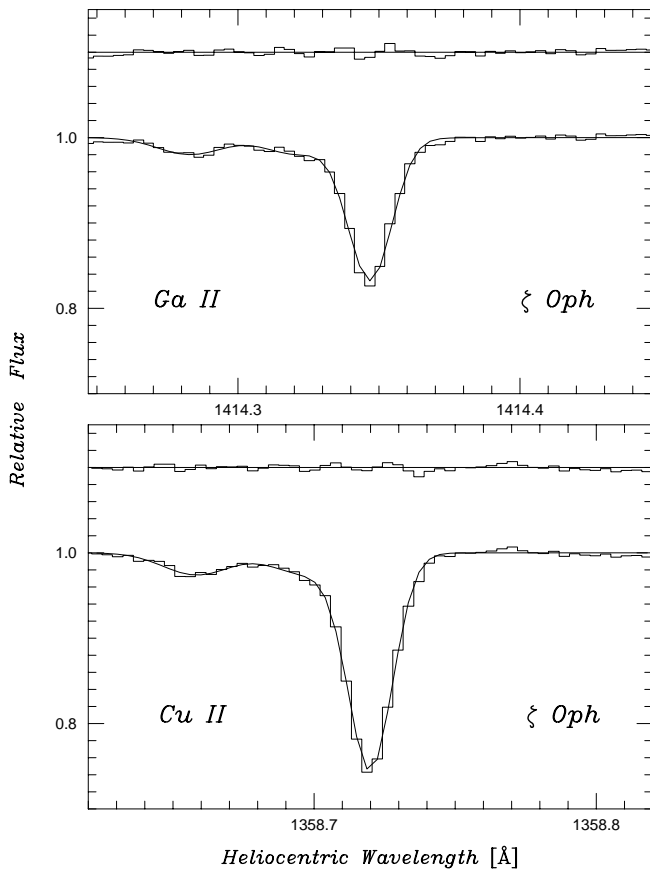


FIG. 2.—Interstellar lines of Ga II and Cu II of  $\zeta$  Oph shown relative to the rectified continuum. The solid line is the fitted profile corresponding to the parameters listed in Table 3. The upper plot in each panel shows the difference between observed and fitted profiles. The weak component to shorter wavelengths of the main two blended components is not included in Table 3.

TABLE 4  
THE  $^{11}\text{B}/^{10}\text{B}$  RATIOS

STAR	$^{11}\text{B}/^{10}\text{B}^a$		
	Ga	Cu	Average
$\zeta$ Oph.....	$4.0 \pm 2.5$	$4.7 \pm 2.8$	$4.3 \pm 1.8$
$\kappa$ Ori.....	$3.2 \pm 1.6$	$3.4 \pm 1.7$	$3.3 \pm 1.2$
$\delta$ Sco.....	$3.8 \pm 1.5$	$2.8 \pm 1.2$	$3.2 \pm 0.9$

<sup>a</sup> Independent determinations using the Ga II and Cu II profiles as templates are listed in columns “Ga” and “Cu,” respectively. The weighted average of the two determinations is also listed.

procedure using the Cu template. The other two profiles were computed assuming the same  $^{11}\text{B}/^{10}\text{B}$  profile but for different  $^{11}\text{B}/^{10}\text{B}$  ratios spanning the ratio given by the fitting procedure. The range of  $^{11}\text{B}/^{10}\text{B}$  from 1.8 to 4.8 clearly exceeds the acceptable range, as expected according to error estimates in Table 4 from the fitting procedure.

Interstellar boron was first detected from *Copernicus* scans of  $\kappa$  Ori with Meneguzzi & York (1980) reporting an equivalent width of  $0.9 \pm 0.4 \text{ m}\text{\AA}$  for the 1362  $\text{\AA}$  line. Jura et al. (1996) from GHR spectra with the G160M gave the equivalent width as  $0.6 \pm 0.3 \text{ m}\text{\AA}$ . These two measurements are quite consistent with the present value of  $0.7 \pm 0.2 \text{ m}\text{\AA}$  off a higher resolution spectrum with a superior S/N.

The previous detection of the B II line in the  $\zeta$  Oph spectrum (Federman et al. 1993) obtained using the G160M

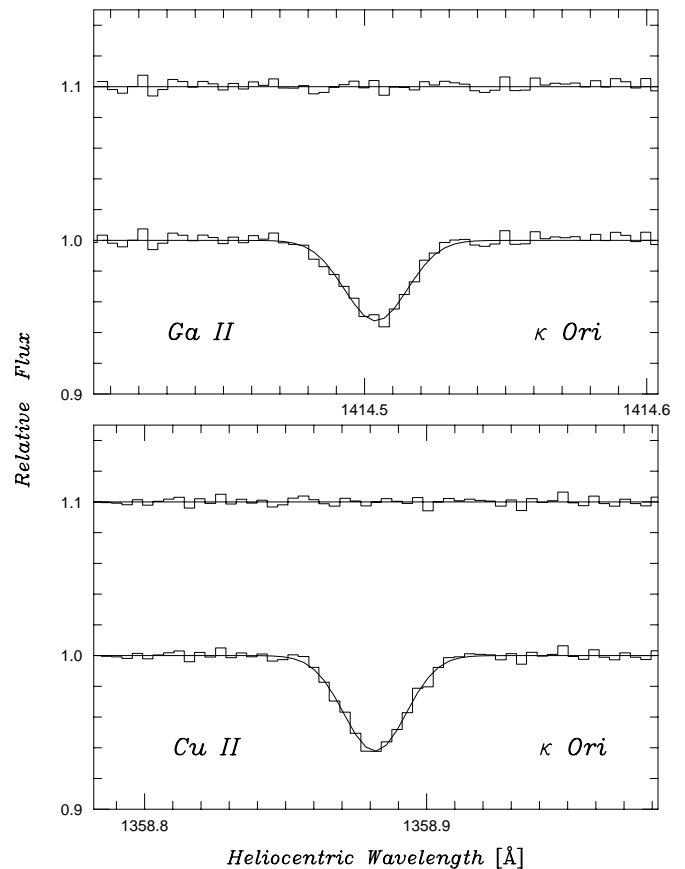


FIG. 3.—Interstellar lines of Ga II and Cu II of  $\kappa$  Ori shown relative to the rectified continuum. See legend to Fig. 2.

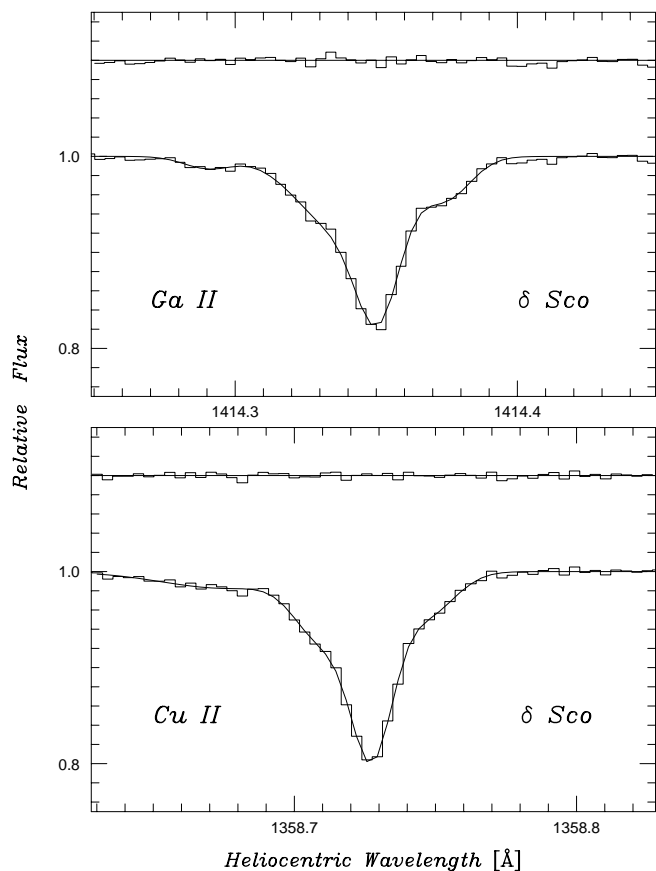


FIG. 4.—Interstellar lines of Ga II and Cu II of  $\delta$  Sco shown relative to the rectified continuum. See legend to Fig. 2. Table 3 lists three components forming the strong line. A fourth but weak component is included here to shorter wavelengths of the main line.

grating gave an equivalent width of  $1.8 \pm 0.3$  mÅ. The present measurement from the echelle spectrum is  $0.6 \pm 0.2$  mÅ, a factor of 3 smaller. Inspection of Figure 1 clearly shows that the line is about half the strength it is in  $\delta$  Sco, i.e., approximately 0.6 mÅ. The earlier higher estimate is presumably a reflection of the lower resolution and an unfortunate presence of incompletely canceled photo cathode granularity. The present measurements of the Cu II and Ga II lines ( $6.4 \pm 0.5$  mÅ and  $4.4 \pm 0.3$  mÅ, respectively) are consistent with the measurements ( $6.6 \pm 0.6$  mÅ and  $3.8 \pm 0.6$  mÅ, respectively) reported by Cardelli, Savage, & Ebbets (1991) off lower S/N echelle spectra. For  $\zeta$  Oph, the equivalent widths of the Cu II and Ga II lines in Table 2 include a small contribution from a weak component (see Fig. 2) well resolved from the main component corresponding to the detected B II line.

The velocities of the components may be checked against published measurements of the same or similar lines. In particular, Savage, Cardelli, & Sofia (1992) present heliocentric velocities derived from ECH-A spectra of the Cu II and Ga II lines. A close reading of their paper shows the intricate steps needed to extract accurate velocities from such spectra. More particularly, a final correction of  $-1.9$  km s $^{-1}$  to the zero point was made empirically using telluric N I lines. Lacking the telluric lines, no great emphasis is placed here on the derived velocities. It suffices to remark that the Cu II 1358 Å line provides the zero point for the B II 1362 Å line. Since the dispersion is known accurately from

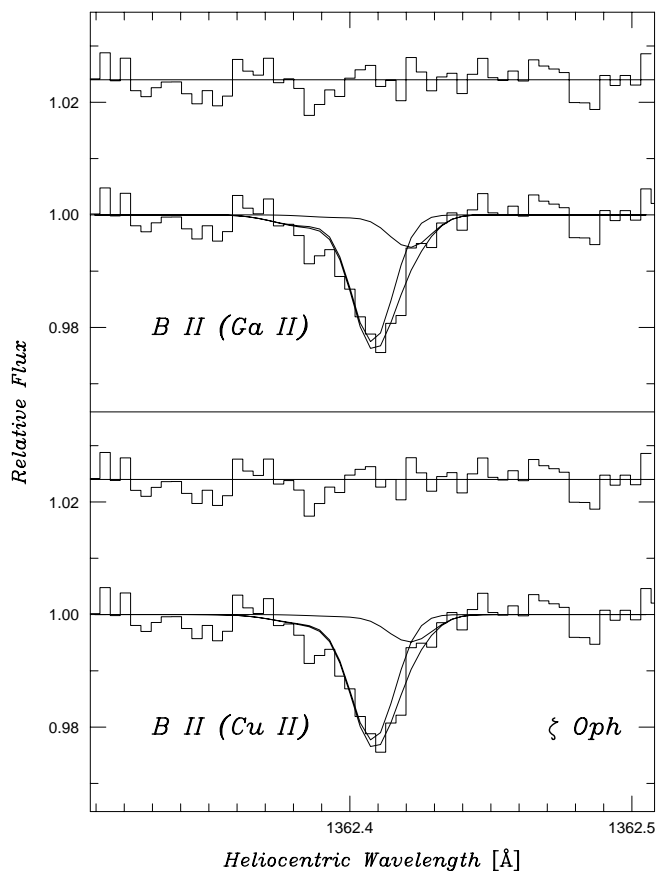


FIG. 5.—The interstellar B II line in  $\zeta$  Oph fitted using the Ga II template (upper panel) and the Cu II template (lower panel). Fitted contributions of the  $^{11}\text{B}$  and  $^{10}\text{B}$  lines—the  $^{10}\text{B}$  line is the weaker component—and their sum are shown. The upper plot in each panel shows the difference between the observed and fitted profiles.

calibration spectra, use of the Cu II line enables an accurate velocity scale to be placed around the B II line.

#### 4. THE INTERSTELLAR BORON ABUNDANCE

Ingredients in the estimation of the boron abundance are the B $^+$ , H I, and H $_2$  column densities. These are tabulated in Table 5 for the three stars of the present paper, as well as  $\lambda$  Ori and  $\iota$  Ori observed by Jura et al. (1996). Several assumptions are implicit in the estimation of  $\log \epsilon(\text{B})$ , namely, all boron in the gas is singly ionized even in the denser parts of clouds where hydrogen is molecular, and the boron abundance is the same in each component when more than a single component is detected in the profiles and that no B $^+$  exists in H II regions along the line of sight. It is not inconceivable that the boron abundance varies from cloud to cloud; for example, if a cloud is mixed with the wind off a star, the boron abundance should be reduced because the stellar surface feeding the wind will be depleted in boron. It is unlikely that the depletion is isotopically dependent: the measured  $^{11}\text{B}/^{10}\text{B}$  ratio is that of the interstellar cloud as a whole.

The present summary of the interstellar B abundance differs in one detail from earlier summaries (Jura et al. 1996; Cunha et al. 1997): the new equivalent width of the 1362 Å line for  $\zeta$  Oph is considerably smaller than Federman et al.'s (1993) value used previously. While the previous summaries concluded that the B abundance was constant across the

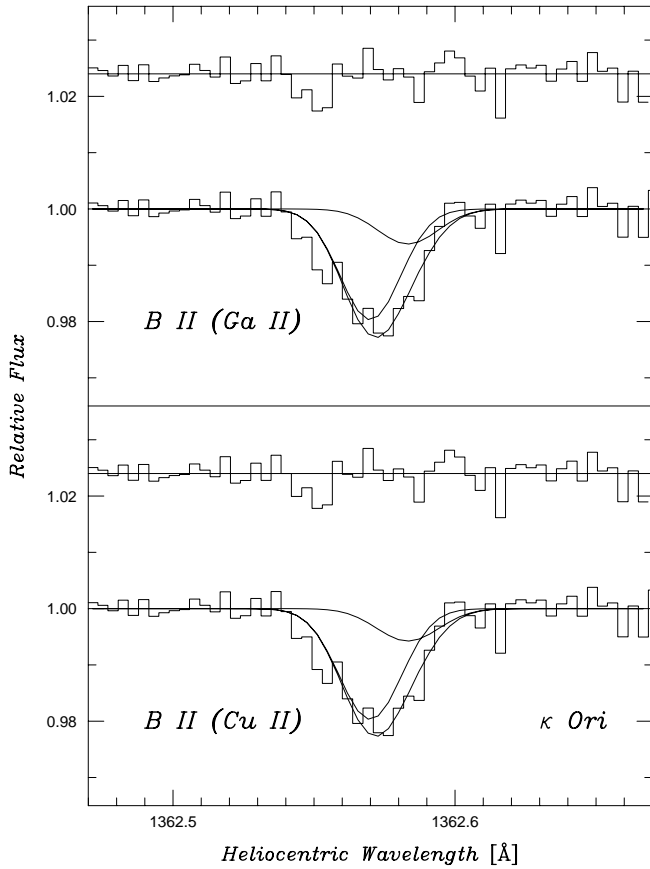


FIG. 6.—The interstellar B II line in  $\kappa$  Ori fitted using the Ga II template (upper panel) and the Cu II template (lower panel). See legend to Fig. 5.

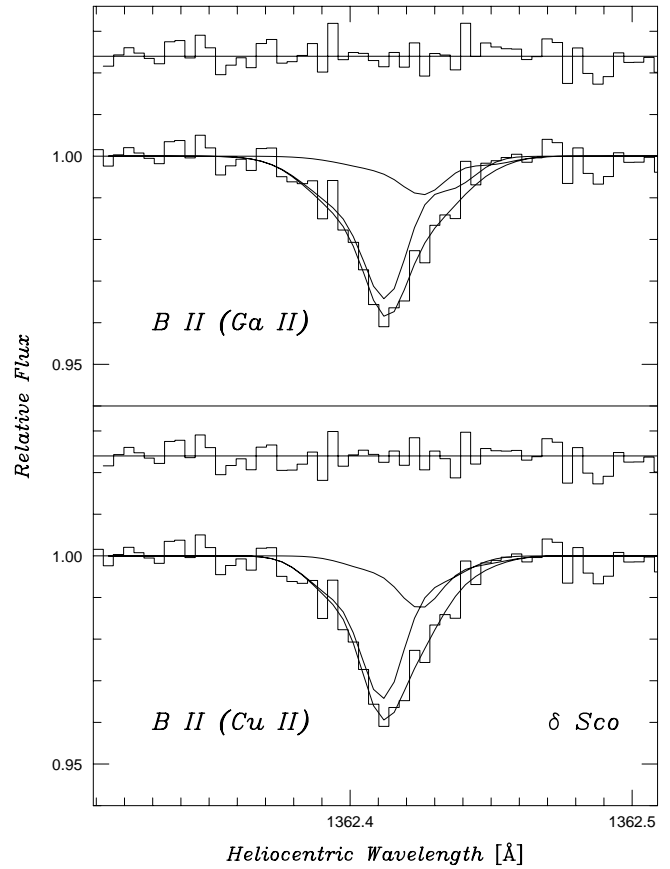


FIG. 7.—The interstellar B II line in  $\delta$  Sco fitted using the Ga II template (upper panel) and the Cu II template (lower panel). See legend to Fig. 5.

small sample, the new results show the  $\zeta$  Oph clouds to have a lower B abundance. The  $\delta$  Sco clouds may also have a lower B abundance than the remaining clouds. It appears now that the B abundance may correlate with the  $\text{H}_2$  fraction and the reddening  $[E(B-V)]$ . The B abundance in the least reddened lines of sight ( $\lambda$  and  $\kappa$  Ori) is  $\log \epsilon(\text{B}) = 2.0$ .

In assessing the B depletion, a problem arises in that little is known about stellar boron abundances. A standard reference is the meteoritic abundance: the most recent estimate is  $\log \epsilon(\text{B}) = 2.78 \pm 0.05$  (Zhai & Shaw 1994), a result consistent with the photospheric abundance,  $\log \epsilon(\text{B}) = 2.6 \pm 0.3$  determined from the blended strong B I line at 2497 Å (Kohl, Parkinson, & Withbroe 1977) and cor-

rected for the minor ( $<0.1$  dex) non-LTE effects (Kiselman & Carlsson 1996). Stellar B abundances first provided by Boesgaard & Heacox (1978) from *Copernicus* scans of the B II 1362 Å line in hot stars gave a mean LTE abundance of  $\log \epsilon(\text{B}) = 2.1 \pm 0.3$  and an estimated non-LTE abundance of 2.3. New non-LTE calculations (Cunha et al. 1997) show that the B abundance for this stellar sample is  $2.7 \pm 0.3$ . *HST* observations of the 1362 Å line in four B stars from the Orion association give a mean non-LTE abundance of  $2.7 \pm 0.2$ . These stellar abundances corrected for the non-LTE effects are in good agreement with the meteoritic abundance and suggests an abundance of about 2.7 as the reference against which to judge interstellar depletions.

TABLE 5  
INTERSTELLAR BORON ABUNDANCES

Star	$\log N(\text{B}^+)^a$ ( $\text{cm}^{-2}$ )	$\log N(\text{H I})^b$ ( $\text{cm}^{-2}$ )	$\log N(\text{H}_2)^c$ ( $\text{cm}^{-2}$ )	$\log N(\text{H})_t^d$ ( $\text{cm}^{-2}$ )	$\log \epsilon(\text{B})^e$
$\lambda$ Ori .....	10.79	20.69	19.11	20.69	2.0
$\iota$ Ori .....	$<10.30$	20.20	14.69	20.20	$<2.1$
$\kappa$ Ori .....	10.63	20.60	15.68	20.60	2.0
$\delta$ Sco .....	10.93	21.01	19.41	21.03	1.9
$\zeta$ Oph .....	10.59	20.69	20.65	21.14	1.5

<sup>a</sup> Taken from Table 2 for  $\kappa$  Ori,  $\delta$  Sco, and  $\zeta$  Oph. Computed from  $W_\lambda$  (1362 Å) given by Jura et al. 1996 for  $\lambda$  Ori and  $\iota$  Ori.

<sup>b</sup> From Diplas & Savage 1994.

<sup>c</sup> From Savage et al. 1977.

<sup>d</sup>  $N(\text{H})_t = N(\text{H I}) + 2N(\text{H}_2)$ .

<sup>e</sup>  $\log \epsilon(\text{B}) = \log N(\text{B}^+)/N(\text{H})_t + 12$ .

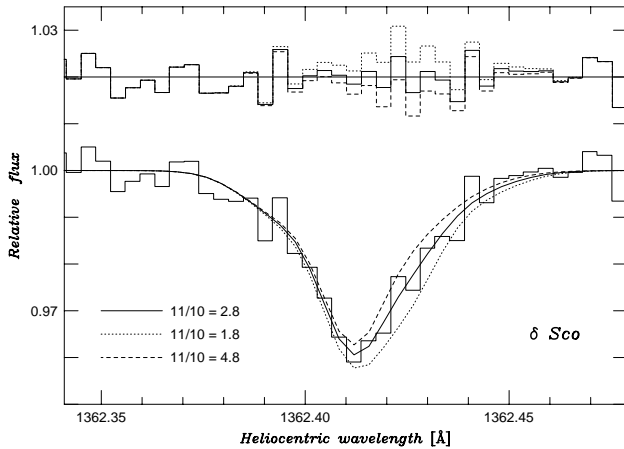


FIG. 8.—The interstellar B II line in  $\delta$  Sco. Three predicted profiles are shown. The solid line is the best fit obtained using the Cu II template (see Fig. 7) and the isotopic ratio  $^{11}\text{B}/^{10}\text{B} = 2.8$ . The other two predictions are variants of the best fit with the  $^{11}\text{B}$  contribution kept constant and the  $^{10}\text{B}$  contribution adjusted to give ratios  $^{11}\text{B}/^{10}\text{B}$  of 2.8 and 4.8. Plots of the difference between the observed and predicted profiles at the top of the figure show that the alternatives are at the limit of acceptability.

This suggestion is not fully confirmed by analyses of the B I 2497 Å line in F and G dwarfs of approximately solar metallicity. The first such analyses by Lemke, Lambert, & Edvardsson (1993) for  $\theta$  UMa and  $\iota$  Peg gave LTE abundances of  $\log \epsilon(\text{B}) = 2.3$  and 2.4, respectively, which Kiselman & Carlsson (1996) correct to recommended non-LTE abundances of 2.4 and 2.6. The difference between the mean (2.5) abundance and the above suggested (2.7) abundance seems insignificant. More recent analyses, however, of these and other F dwarfs have suggested lower abundances. Boesgaard et al. (1997) give a mean non-LTE abundance of 2.1 from several stars including the pair analyzed by Lemke et al. This abundance is about 0.7 dex less than the meteoritic abundance. At present, the various abundance estimates cannot be reconciled. Speculations may be advanced: systematic errors lead to an overestimate of the meteoritic abundance, the non-LTE corrections to the stellar B II 1362 Å line are overestimated [the LTE abundances are close to  $\log \epsilon(\text{B}) = 2.0$ ], the difficulties in analyzing the B I line in F dwarfs have been underestimated. For the present, the apparently irreconcilable abundance estimates are noted and an additional clue is sought in the interstellar abundances of Cu and Ga.

Estimates of the Cu and Ga depletions are made using the integrated profiles; i.e., the possibility of different depletions in different components is ignored. There is a practical reason for adopting the assumption: available measures of the H I and H<sub>2</sub> column density lack the spectral resolution to provide column densities for individual components. In the case of  $\zeta$  Oph, Savage et al. (1992) found elements to be quite substantially less depleted in the  $-27 \text{ km s}^{-1}$  component than in the cool  $-15 \text{ km s}^{-1}$  component. The present analysis refers to the  $-15 \text{ km s}^{-1}$  component. The much weaker  $-27 \text{ km s}^{-1}$  component is well resolved (Fig. 2) and is not included in the procedures used to match a synthetic profile to the observed profile. Savage et al. argue that the hydrogen column density is overwhelmingly associated with the  $-15 \text{ km s}^{-1}$  component. In this one case, the distinction between components is not crucial to the argument. In the event that a line of sight intersects an H II

region, a depletion will be an upper limit to the true depletion unless the ion of relevance is not present in the H II region. In order of increasing  $E(B-V)$  the Cu depletions relative to the solar system abundance [ $\log \epsilon(\text{Cu}) = 4.27$ ; Anders & Grevesse 1989] are (in dex)  $-1.4$  ( $\kappa$  Ori),  $-1.2$  ( $\delta$  Sco), and  $-1.3$  ( $\zeta$  Oph). Savage & Sembach (1996) give a depletion of  $-1.5$  dex for  $\zeta$  Per's cool cloud, which resembles that in front of  $\zeta$  Oph. Depletions for Ga relative to the solar system abundance [ $\log \epsilon(\text{Ga}) = 3.13$ ; Anders & Grevesse 1989] are  $-1.1$  ( $\kappa$  Ori),  $-0.8$  ( $\delta$  Sco), and  $-1.1$  ( $\zeta$  Oph). These results for Cu and Ga suggest that, to within the errors of measurement, the depletion is roughly constant over this selection of clouds. Even in very lightly reddened clouds depletions of about  $-1$  dex are experienced.

A parameter often invoked as a substitute for knowledge of the chemistry is the condensation temperature,  $T_c$ , which is the temperature at which 50% of an element has condensed into grains in gas at a pressure of  $10^{-4}$  atm and with a solar mix of elements. Estimated values of  $T_c$  are 1037 K and 918 K for Cu and Ga, respectively (Savage & Sembach 1996). The  $T_c$  assigned to B by Federman et al. (1993) and Savage & Sembach (1996) is  $T_c = 650$  K from Field (1974). Recent calculations indicate a higher  $T_c$  with Zhai (1995) and Lauretta & Lodders (1996) giving 910 K and 964 K, respectively. These estimates suggest that B, Cu, and Ga should be depleted by similar factors. Then, the total B abundance for lightly reddened lines of sight is expected to be about 1 dex higher than the observed abundance of 2.0; i.e., the total abundance is close to the meteoritic abundance of 2.8.

Although  $T_c$  now points to Cu and Ga as suitable calibrators for the B depletion, it must be noted that plots of depletion versus  $T_c$  show considerable spread; for example, the depletions for the  $-15 \text{ km s}^{-1}$  component of  $\zeta$  Oph show a 1 dex spread at all  $T_c$  from 500 to 1500 K (Savage & Sembach 1996, Fig. 4). Cardelli (1994) has stressed that other factors are at work. Therefore, additional insights into the chemistry of gas and grains will be needed to use the abundance of boron in interstellar gas to establish unequivocally the total abundance.

## 5. THE BORON ISOTOPIC RATIO

Results for the  $^{11}\text{B}/^{10}\text{B}$  ratio are summarized in Table 4. To within the measurement errors, the three lines of sight give the same ratio. A grand mean is obtained by weighting the individual results by the inverse of their estimated uncertainty. This average is  $^{11}\text{B}/^{10}\text{B} = 3.4 \pm 0.7$ . This result is probably larger than the ratio ( $=2.5$ ) predicted for boron production by spallation driven by high-energy galactic cosmic rays and the observed ratio ( $=2.52 \pm 0.20$ ; Mewaldt 1989; Gibner et al. 1992) in those cosmic rays. The standard isotopic ratio for solar system material is close to 4.0. Anders & Grevesse (1989) give the ratio as 4.02. Chaussidon & Robert (1995) report on a variation of the isotopic ratio in meteoritic chondrules from four different chondritic meteorites. The variation from 3.84 to 4.25 was attributed to inhomogeneities in the gas that comprised the solar nebula and from which meteorites formed. Zhai et al. (1996) found a much smaller variation (4.011–4.098) for bulk samples from 32 meteorites.

To within the errors of measurement, the isotopic ratios of the local interstellar medium and the solar system are identical. The usual interpretation of such a concordance is

that the ratio has not evolved over the 4.5 Gyr since the formation of the solar system. This statement, however, supposes that the galactic neighborhood of the Sun has evolved as a “closed box.” It is by no means apparent that this is the case; for example, interstellar gas and local young stars seem to be deficient in oxygen (and other elements) relative to the Sun (Meyer et al. 1994; Cardelli et al. 1996; Kilian 1992; Gies & Lambert 1992; Cunha & Lambert 1994), a fact at odds with chemical evolution of a closed box. Resolutions of this difficulty have been proposed including infall and the migration of the Sun outward from its birthplace.

Here, comment is restricted to the relation between the observed and predicted ratios for the boron isotopic ratio and related elemental and isotopic abundance ratios. The elements of primary concern are Li, Be, and B.<sup>3</sup> It is well known that spallation driven by high-energy galactic cosmic rays accounts rather well for the solar system mix of  $^6\text{Li}$ ,  $^9\text{Be}$ , and  $^{10}\text{B}$ , but spallation produces less than the observed amounts of  $^7\text{Li}$  and  $^{11}\text{B}$ . Supplements of these two nuclides may be contributed by stars. Neutrino-induced spallation (the  $\nu$ -process) occurring in Type II supernovae is predicted to contribute both nuclides in roughly the desired ratio (Woosley et al. 1990; Woosley & Weaver 1995) and at a rate adequate to build the abundances up to their level in the solar system and young stars (Timmes, Woosley, & Weaver 1995). The  $\nu$ -process does not appear to produce  $^6\text{Li}$ ,  $^9\text{Be}$ , and  $^{10}\text{B}$  in significant amounts. Lithium as  $^7\text{Li}$  may be synthesized by red giants that convert  $^3\text{He}$  made in the main sequence progenitor to  $^7\text{Li}$  at a time when the giant has a “hot bottom convective envelope.” Observations and predictions regarding this mode of synthesis are in fair agreement (Sackmann & Boothroyd 1992; Smith et al. 1995). These red giants do not synthesize the other nuclides in the Li, Be, and B group. Low-energy cosmic rays may supplement the products from spallation by high-energy cosmic rays. The big bang produces  $^7\text{Li}$  at about the level seen in warm halo dwarfs whose atmospheres may retain the primordial lithium abundance. Big bang production of  $^6\text{Li}$ ,  $^9\text{Be}$ ,  $^{10}\text{B}$ , and  $^{11}\text{B}$  is predicted to be at orders of magnitude below the abundances reported for halo dwarfs.

A recent ingredient into the discussions is the inferred presence of low-energy (about 10 MeV nucleon<sup>-1</sup>) C and O nuclei in the Orion association. Bloemen et al. (1994) identify this localized low-energy cosmic-ray flux from detection of  $\gamma$ -ray lines produced by excited C and O nuclei—but see Murphy et al. (1996). These C and O nuclei may be the agent needed to supplement the products from high-energy cosmic-ray spallation such that the  $^{11}\text{B}/^{10}\text{B}$  and B/Be ratios are increased to the observed values. Ramaty, Kozlovsky, & Lingenfelter (1996) provide a detailed discussion of the yields from spallation by low-energy cosmic rays. Variations of energy spectrum, cosmic ray composition, and com-

position of the interstellar medium are investigated. It is found, not unexpectedly in light of earlier work, that plausible combinations of energy spectrum, cosmic ray and interstellar composition can account for the relative abundances of  $^6\text{Li}$ ,  $^9\text{Be}$ ,  $^{10}\text{B}$ , and  $^{11}\text{B}$  but not  $^7\text{Li}$  which is, in general, underproduced. The  $^7\text{Li}/^6\text{Li}$  ratio (= 12.5) of the solar system is reproduced if there is a large flux of low-energy ( $\leq 10$  MeV nucleon<sup>-1</sup>) cosmic rays, but the efficiency of production is low and an inordinate amount of energy has to be given to the cosmic rays.<sup>4</sup> Since  $^7\text{Li}$  seems to require a stellar source to supplement a pregalactic contribution from the big bang and the production by cosmic rays, interstellar  $^7\text{Li}/^6\text{Li}$  and  $^{11}\text{B}/^{10}\text{B}$  ratios are not simply coupled in a unified interpretation.

In short, a scenario invoking the presence of low-energy Orion-like cosmic rays can plausibly account for the relative abundances of the Li, Be, and B nuclides, except for  $^7\text{Li}$ , which is underproduced by a factor of about 5. If this scenario is correct, a stellar supplement of  $^7\text{Li}$  would suffice for complete accounting. Lithium-rich red giants are a promising source of  $^7\text{Li}$ . A large supplement from Type II supernovae is excluded as the  $\nu$ -process is predicted to make both  $^7\text{Li}$  and  $^{11}\text{B}$  in roughly solar proportions. Of course, if the contribution from low-energy cosmic rays were reduced, a supernova contribution would be required. There is, however, tentative evidence from the relative abundance of Be and B in unevolved stars that B is primarily a product of spallation. Boesgaard & King (1993) showed that the Be abundance at a fixed iron abundance varied by about 0.8 dex for stars of near solar metallicity. Boesgaard et al. (1997) show that B probably follows Be such that the B/Be is constant. Since Be is solely a product of spallation, it follows that B is probably also a spallation product, especially as the B/Be ratio is about that expected for spallation. On the other hand, if B were a product of Type II synthesis, the B/Be ratio should vary quite considerably.

## 6. CONCLUDING REMARKS

On the introduction of high-energy cosmic rays as an agent of element production, it was evident that the solar system's isotopic boron ratio was inconsistent with the predicted yields. An overabundance of  $^7\text{Li}$  was similarly noted as an inconsistency. As long as the solar system was the sole source of the measured  $^{11}\text{B}/^{10}\text{B}$  ratio (= 4.05), a suspicion lingered that it was an anomaly and that the prediction,  $^{11}\text{B}/^{10}\text{B} \approx 2.5$ , for spallation by high-energy cosmic rays was satisfied elsewhere in the Galaxy. Measurements discussed here show that the solar ratio is likely to be representative of the local galactic neighborhood. Introduction of low-energy cosmic rays can reconcile the observed and predicted isotopic ratios. Detection of  $\gamma$ -ray line emission from the Orion association is evidence of the presence of the required low-energy cosmic rays. Then, the nucleosynthesis of the boron isotopes would seem to be understood. In particular, a stellar source seems not to be required. Such a source is needed to account for the observed  $^7\text{Li}$  abundance.

<sup>3</sup> Comparison of elemental ratios for interstellar gas are bedeviled by the depletion onto grains and the fact that depletions, even relative depletions, are unknown (a priori). In principle, this difficulty may be bypassed by using the abundances measured for young stars whose Li, Be, and B abundances, in the absence of internal destruction or diffusion, will be identical to those of the present interstellar gas. The Li and Be elemental abundances in unevolved stars of near solar metallicity are similar to those of the meteorites (cf. Cunha et al. 1997 for Li; Boesgaard & King 1993 for Be). It is likely that the stellar B abundances also match the meteoritic value but this is not yet definitively established.

<sup>4</sup> Interstellar  $^7\text{Li}/^6\text{Li}$  ratios have been measured. Lemoine, Ferlet, & Vidal-Madjar (1995) give  $^7\text{Li}/^6\text{Li} = 11 \pm 2$  and  $8.9 \pm 2$  for the principal clouds along the line of sight to  $\rho$  Oph and  $\zeta$  Oph, respectively. These are slightly less than the solar system ratio. In a second cloud along each line of sight, a much lower ratio (3.4 and 1.4) was indicated. These lower ratios are consistent with production by spallation. See also Meyer, Hawkins, & Wright (1993).



Li-rich red giants satisfy the condition that the stellar source produce lithium (as  ${}^7\text{Li}$ ) but not boron or beryllium. Type II supernovae, which may compete with red giants as a source of  ${}^7\text{Li}$ , are predicted to make  ${}^{11}\text{B}$  and  ${}^{19}\text{F}$  too. If the flux of low-energy cosmic rays is shown to be substantially less than presently considered, Type II supernovae may need to be invoked to supplement the spallation products of high-energy cosmic rays. Observations of QSO absorption-line systems may provide data on the abundances of some of the products from cosmic-ray interactions with interstellar nuclei in young galaxies. In the case of  ${}^{19}\text{F}$  such data is unavailable from spectroscopy of metal-

poor halo stars. A program to establish more firmly the boron abundance of local young stars may better define the depletion of boron in the interstellar medium. In turn, this datum will be an additional clue in the search for the physics behind the depletion of elements in interstellar gas.

This research is made possible through grants from the Space Telescope Science Institute to the University of Texas, the University of Toledo, and Villanova University. The support of the R. A. Welch Foundation of Houston, Texas, is also gratefully acknowledged.

## REFERENCES

- Anders, E., & Grevesse, N. 1989, *Geochim. Cosmochim. Acta*, 53, 197  
 Bloemen, H., et al. 1994, *A&A*, 281, L5  
 Boesgaard, A. M., Deliyannis, C. P., Stephens, A., & Lambert, D. L. 1997, *ApJ*, 492, 727  
 Boesgaard, A. M., & Heacox, W. D. 1978, 226, 8888  
 Boesgaard, A. M., & King, J. R. 1993, *AJ*, 106, 2309  
 Cardelli, J. A. 1994, *Science*, 265, 209  
 Cardelli, J. A., & Ebbets, D. C. 1994, in *Calibrating Hubble Space Telescope, HST Calibration Workshop*, ed. J. C. Blades & S. J. Osmer (Baltimore: STScI), 322  
 Cardelli, J. A., Meyer, D. M., Jura, M., & Savage, B. D. 1996, *ApJ*, 467, 334  
 Cardelli, J. A., Savage, B. D., & Ebbets, D. C. 1991, *ApJ*, 383, L23  
 Chaussidon, M., & Robert, F. 1995, *Nature*, 374, 337  
 Cunha, K., & Lambert, D. L. 1994, *ApJ*, 426, 170  
 Cunha, K., Lambert, D. L., Lemke, M., Gies, D. R., & Roberts, L. M. 1997, *ApJ*, 478, 211  
 Diplas, A., & Savage, B. D. 1994, *ApJS*, 93, 211  
 Federman, S. R., Lambert, D. L., Cardelli, J. A., & Sheffer, Y. 1996, *Nature*, 381, 764  
 Federman, S. R., Sheffer, Y., Lambert, D. L., & Gilliland, R. L. 1993, *ApJ*, 413, L51  
 Field, G. B. 1974, *ApJ*, 187, 453  
 Gibner, P. S., Mewaldt, R. A., Schindler, S. M., Stone E. C., & Webber, W. R. 1992, *ApJ*, 391, L89  
 Gies, D. R., & Lambert, D. L. 1992, *ApJ*, 387, 673  
 Jura, M., Meyer, D. M., Hawkins, I., & Cardelli, J. A. 1996, *ApJ*, 456, 598  
 Jönsson, P., Johansson, S. G., & Froese Fischer, C. 1994, *ApJ*, 429, L45  
 Kilian, J. 1992, *A&A*, 262, 171  
 Kiselman, D., & Carlsson, M. 1996, *A&A*, 311, 680  
 Kohl, J. L., Parkinson, W. H., & Withbroe, G. L. 1977, *ApJ*, 212, L101  
 Lauretta, D. S., & Lodders, K. 1996, *Meteorit. Planet. Sci.*, 31 (Suppl.), A77  
 Lemke, M., Lambert, D. L., & Edvardsson, B. 1993, *PASP*, 105, 468  
 Lemoine, M., Ferlet, R., & Vidal-Madjar, A. 1995, *A&A*, 298, 879  
 Meneguzzi, M., Audouze, J., & Reeves, H. 1971, *A&A*, 15, 337  
 Meneguzzi, M., & Reeves, H. 1975, *A&A*, 40, 99  
 Meneguzzi, M., & York, D. G. 1980, *ApJ*, 235, L111  
 Mewaldt, R. A. 1989, in *AIP Conf. Proc.* 183, *Cosmic Abundances of Matter*, ed. C. J. Waddington (New York: AIP), 124  
 Meyer, D. M., Hawkins, I., & Wright, E. L. 1993, *ApJ*, 409, L61  
 Meyer, D. M., Jura, M., Hawkins, I., & Cardelli, J. A. 1994, *ApJ*, 437, L59  
 Morton, D. C. 1991, *ApJS*, 77, 119  
 Murphy, R. J. et al. 1996, *ApJ*, 473, 990  
 Ramaty, R., Kozlovsky, B., & Lingenfelter, R. E. 1996, *ApJ*, 456, 525  
 Reeves, H. 1974, *ARA&A*, 12, 437  
 Reeves, H., Fowler, W. A., & Hoyle, F. 1970, *Nature*, 226, 727  
 Sackmann, J.-I., & Boothroyd, A. I. 1992, *ApJ*, 392, L71  
 Savage, B. D., Bohlin, R. C., Drake, J. F., & Budich, W. 1977, *ApJ*, 216, 291  
 Savage, B. D., Cardelli, J. A., & Sofia, U. 1992, *ApJ*, 401, 706  
 Savage, B. D., & Sembach, K. R. 1996, *ARA&A*, 34, 279  
 Smith, V. V., Plez, B., Lambert, D. L., & Lubowich, D. A. 1995, *ApJ*, 441, 735  
 Timmes, F. X., Woosley, S. E., & Weaver, T. A. 1995, *ApJS*, 98, 617  
 Woosley, S. E., Hartmann, D. H., Hoffmann, R. D., & Haxton, W. C. 1990, *ApJ*, 356, 272  
 Woosley, S. E., & Weaver, T. A. 1995, *ApJS*, 101, 181  
 Zhai, M. 1995, *Meteoritics*, 30, 733  
 Zhai, M., Nakamura, E., Shaw, D. M., & Nakano, T. 1996, *Geochim. Cosmochim. Acta*, 60, 4877  
 Zhai, M., & Shaw, D. M. 1994, *Meteoritics*, 29, 607